Earth and Planetary Science Letters 366 (2013) 71–82

Contents lists available at SciVerse ScienceDirect

Earth and Planetary Science Letters

journal homepage: www.elsevier.com/locate/epsl

Magmatic evolution and crustal recycling for Neoproterozoic strongly peraluminous granitoids from southern China: Hf and O isotopes in zircon

Xiao-Lei Wang [a,b,*], Jin-Cheng Zhou [a], Yu-Sheng Wan [c], Kouki Kitajima [b], Di Wang [a], Chloe Bonamici [b], Jian-Sheng Qiu [a], Tao Sun [a]

[a] State Key Laboratory for Mineral Deposits Research, School of Earth Science and Engineering, Nanjing University, Nanjing 210093, China
[b] WiscSIMS, Department of Geoscience, University of Wisconsin, 1215 W. Dayton Street, Madison, Wisconsin 53706, USA
[c] Beijing SHRIMP Center, Institute of Geology, Chinese Academy of Geological Sciences, Beijing 100037, China

ARTICLE INFO

Article history:
Received 7 November 2012
Received in revised form
12 February 2013
Accepted 12 February 2013
Editor: T.M. Harrison
Available online 19 March 2013

Keywords:
Hf and O isotopes
clearly defined cores
zircon
S-type granitoids
magmatic evolution
Jiangnan orogen

ABSTRACT

Zircons can retain a grain-scale record of granitoid compositional evolution that is accessible through microanalysis. *In situ* U–Pb, Hf and O isotope data yield new insights into the petrogenesis and evolution of the Neoproterozoic strongly peraluminous granitoids of the Jiangnan orogen (JO), southern China. A negative correlation of Th/U *versus* $\delta^{18}O$ is found for most analyses. Some zircons from eastern JO granitoids show $\delta^{18}O$ variations of 3–6‰ from core to rim, indicating a dramatic shift toward higher oxygen isotope values by voluminous partial melting of supracrustal rocks and signaling a transition from I-type-like to S-type-like magmas during the later stage of magmatic evolution. This mechanism provides a reasonable explanation why some granitoids have intermediate geochemical features between S-type and I-type granites. Hf isotope trends indicate that a larger proportion of mature continental crust was incorporated into the magma sources of the western JO granitoids, whereas more juvenile arc crust was incorporated into the eastern JO magmas. No significant depleted mantle-derived mafic magma was injected into the JO granitoid magmas. Instead, radiogenic Hf and Nd signatures in JO granitoids reflect incorporated juvenile arc crust and document crustal growth in southern China during the Early Neoproterozoic (*ca.* 900 Ma). Thus, our zircon data suggest that strongly peraluminous granitoids, which are widely regarded as the products of orogenesis that primarily recycle evolved crust, can also record important information about early crustal growth.

1. Introduction

Understanding the processes that govern the evolution of continental crust from formation to destruction is a major goal in Earth sciences. As the final magmatic products of mantle–crust evolution, granitoids (or granitic rocks) constitute an essential part of continental crust. Extraction of granite from lower crust and emplacement at shallower levels is the principal mechanism of continental differentiation (Solar et al., 1998). The origins and petrogenesis of granitoids are therefore essential to understanding the evolution of continental crust.

Experimental results suggest that granitoids are not generally formed directly from melting of mantle peridotite (Johannes and Holtz, 1996), but rather from the partial melting of diverse crustal rocks, including mantle-derived juvenile mafic rocks, recycled sedimentary rocks, or pre-existing igneous rocks (including other granites). Nonetheless, questions about the input of mantle-derived magmas into the granite source persist (Collins, 1996; Yang et al., 2004) because the mantle and mantle-derived melts are thought to be the dominant heat source for partial melting in the crust (Clemens, 2003). The complexity of magma sources precludes a simple explanation of the significance of granitoids on the crustal growth and evolution (*e.g.*, Kemp et al., 2007).

Two broad compositional classes of granitoids, S-type (sedimentary) and I-type (igneous), were proposed by White and Chappell (1977) based on studies of the Lachlan Fold Belt (LFB). S- and I-type granitoids are attributed to the partial melting of fundamentally compositionally different crustal source rocks—metasedimentary and metaigneous, respectively. However, a recent study of LFB I-type granitoids showed high oxygen isotope values consistent with reworking of sediments by mantle-like magmas (Kemp et al., 2007), and thus suggests overlap in the sources of I- and S-type granitoids (Clemens, 2003). Therefore, in order to better understand crustal differentiation and magmatic evolution, the petrogenesis of S-type granitoids and their relationship with I-type rocks need further study.

S-type granitoids are strongly peraluminous, with aluminum saturation index (ASI = molar $Al_2O_3/(CaO+Na_2O+K_2O)$) greater than 1.1 (White and Chappell, 1977; Clemens, 2003) and the occurrence of aluminum-rich minerals, such as garnet, cordierite,

* Corresponding author at: State Key Laboratory for Mineral Deposits Research, School of Earth Science and Engineering, Nanjing University, Nanjing 210093, China. Tel.: +86 25 89680896; fax: +86 25 83686016.
E-mail addresses: xlwangnju@yahoo.com.cn, wxl@nju.edu.cn (X.-L. Wang).

0012-821X/$ - see front matter © 2013 Elsevier B.V. All rights reserved.
http://dx.doi.org/10.1016/j.epsl.2013.02.011

muscovite, andalusite, and tourmaline. Peraluminous S-type granitoids generally occur in orogenic belts that rework juvenile crust and/or experience partial melting of metasedimentary rocks in the lower to middle crust (Kamei, 2002). S-type granitoids generally have high initial $^{87}Sr/^{86}Sr$ ratios (>0.707) (Chappell and White, 2001) reflecting partial melting of mature continental crust that includes weathered sedimentary rocks with high Rb/Sr ratio and thus higher $^{87}Sr/^{86}Sr$ ratios (Goldstein and Jacobsen, 1988). There are, however, examples of cordierite-bearing "S-type" granitoids that have rather low initial $^{87}Sr/^{86}Sr$ ratios similar to initial $^{87}Sr/^{86}Sr$ typical of I-type granitoids (Clemens, 2003; Wu et al., 2006). Conversely, I-type granitoids may also be peraluminous (Chappell and White, 2001) or have high oxygen isotope ratios (whole-rock $\delta^{18}O$ over 10‰ or zircon $\delta^{18}O$ approaching 9.5‰; Ferreira et al., 2003; Kemp et al., 2007) when weathered components are included in the magma source.

Due to the complexity of magmatic processes that form granitoids, and of subsolidus alteration, bulk rock geochemistry typically fails to reveal the full magmatic and crustal history. Zircon is a common and highly refractory accessory mineral in granitoids that can preserve the isotopic composition of its parent magma at the time of crystallization. There are multiple isotopic systems (*e.g.*, U–Pb, Hf, and O isotopes) in zircon that can be explored through *in situ* microanalysis (Valley, 2003; Hawkesworth and Kemp, 2006; Kemp et al., 2007). Ideally, U–Pb isotopes reveal the crystallization age of granitoids; Hf isotopes indicate the mantle extraction age of the source materials (juvenile crust or recycled old crustal materials); and oxygen isotopes record involvement of material that has experienced surface processes in the source (*i.e.*, if protolith experienced earlier supracrustal processes such as weathering and alteration).

Non-radiation-damaged zircon is extremely retentive of the magmatic oxygen isotope ratio due to the low diffusivity of oxygen even during granulite-facies metamorphism and anatexis (Page et al., 2007; Bowman et al., 2011). Zircons in high-temperature equilibrium with pristine mantle-derived melts fall into a narrow range of $\delta^{18}O$ [5.3 ± 0.6 per mil (‰)] (Valley et al., 2005). This range is insensitive to magmatic differentiation, because the attendant rise in bulk rock $\delta^{18}O$ is compensated by an increase in zircon/magma $\delta^{18}O$ fractionation ($\Delta^{18}O_{magma\text{-}zircon}$) from *ca.* +0.5‰ for mafic melts to +1.5‰ for silicic magma (Valley et al., 2005; Lackey et al., 2008). Values of $\delta^{18}O$ in zircon above ~6.3‰ thus indicate an ^{18}O-enriched crustal component in the magma from which the zircon crystallized. Higher values, above 7.5‰ are attributed to supracrustal sources, most commonly either sedimentary rock ($\delta^{18}O = 10$–30‰) or altered volcanic rock (to 20‰) (Valley et al., 2005). In contrast, zircons with $\delta^{18}O$ lower than the mantle range (<4.5‰) suggest exchange of heated meteoric or sea water with the magma protolith (Valley, 2003). Variations of oxygen isotopes within individual zircons can therefore be used to trace melt inputs during the evolution of S-type granitic magmas. Thus, combined Hf and O isotope data in individual zircon crystals can give detailed genetic information about parent magmas, and, in particular, source characteristics of S-type granitoids.

Neoproterozoic granitoids (mostly S-type) outcrop over 7500 km^2 in the Jiangnan orogen (JO) between the Yangtze Block and the Cathaysia Block, southern China (Fig. 1). Recent *in situ* U–Pb dating of magmatic zircons indicates that most of these granitoids crystallized at 835–800 Ma, with an age peak at *ca.* 820 Ma (X.H. Li et al., 2003; Wang et al., 2006). A few late granitoids intruded at *ca.* 780 Ma (Shi'ershan Pluton; Zheng et al., 2008). All of the granitoids are strongly peraluminous (X.H. Li et al., 2003; Wang et al., 2006; Wu et al., 2006; Zheng et al., 2008), suggesting partial melting of metasedimentary rocks (Chappell and White, 2001). In this study, we report *in situ* U–Pb, Hf, and O isotope analyses for subdomains within zircons of eight Neoproterozoic granitoids of the Jiangnan orogen. Our data show a transition in oxygen isotope compositions from I-type-like to S-type-like and shed light on the genesis of the strongly peraluminous granitoids and related crustal evolution processes. Our work follows previous studies in suggesting that the sources of felsic magmas can be diverse and mixed (*e.g.*, Collins, 1996; Kemp et al., 2007; Miller et al., 1988), but we show that the distinction between I- and S- type granitoids may be blurred even at the scale of individual zircon crystals.

2. Geological background and sample details

Southern China (*i.e.*, the South China Block) is made up of the Yangtze Block to the northwest and the Cathaysia Block to the southeast (Fig. 1A), sutured along the Jiangnan orogen, which comprises mainly Proterozoic metasedimentary and igneous rocks. The Proterozoic metasedimentary sequences are structurally divided into folded sequences and an overlying cover sequences separated by an angular unconformity. The folded metasedimentary sequences may have been deposited in a retro-arc foreland basin setting following arc–continent collision between the Yangtze and Cathaysia blocks (Wang et al., 2007) and subsequently experienced deformation at low-greenschist facies conditions. U–Pb zircon ages in detrital grains from the metasedimentary units and in magmatic grains from interlayered volcanic units indicate that metamorphism occurred at 860–820 Ma (Wang et al., 2007 and our unpublished data). During the later stage of the amalgamation between the Yangtze and Cathaysia blocks, voluminous granitoids intruded the folded sequences. Recently published *in situ* SHRIMP and LA-ICP-MS zircon U–Pb ages suggest that these granitoids were emplaced at *ca.* 835–800 Ma (X.H. Li et al., 2003; Wang et al., 2006), with the exception of the Shi'ershan Pluton (*ca.* 780 Ma; Z.X. Li et al., 2003; Fig. 1c), which intruded the cover sequences and probably represents post-orogenic magmatism (Wang et al., 2012).

The JO Neoproterozoic granitoids are strongly peraluminous. Biotite is the major mafic mineral in all granitoids; no hornblende was observed. Granitoids in the eastern and western segments of the JO show different mineralogical and geochemical characteristics (X.H. Li et al., 2003; Wang et al., 2006; Wu et al., 2006). Garnet and cordierite are common in the granitoids from the eastern segment of the JO, whereas tourmaline and garnet are the common aluminum-rich minerals in the western segment. Granitoids in the eastern JO generally have low whole-rock initial $^{87}Sr/^{86}Sr$ ratios (*ca.* 0.704; Zhou and Wang, 1988) and near-zero $\varepsilon Nd(t)$ values (X.H. Li et al., 2003; Wu et al., 2006; Zheng et al., 2008), despite their high ASI, making their I-/S-type classification ambiguous (Zhou and Wang, 1988; Wu et al., 2006).

We examined zircon crystals in 10 samples from 8 granitic plutons throughout the JO (Table 1): the Xucun (Fig. 1b), Shi'ershan (Fig. 1c) and Jiuling (Fig. 1d) plutons in the eastern segment; and the Yuanbaoshan, Sanfang, Longyou, Bendong and Dongma plutons (Fig. 1e) in the western segment of the JO. Granitoids from the western JO are associated with mafic intrusion (Fig. 1e) dated at *ca.* 820 Ma (Li et al., 1999; Wang et al., 2006). A summary of the ages and petrographic descriptions of the granitoids are given in Table 1. Because the Jiuling Pluton is the largest (3860 km^2), three samples (including one diorite enclave) were selected for study (Fig. 1d; Table 1).

3. Analytical methods

Whole-rock Nd isotopes of the Neoproterozoic granitoids were analyzed using a Neptune (Plus) multiple-collector inductively-coupled plasma mass spectrometer (MC-ICP-MS) at the State Key Laboratory for Mineral Deposits Research (MiDeR), Nanjing University

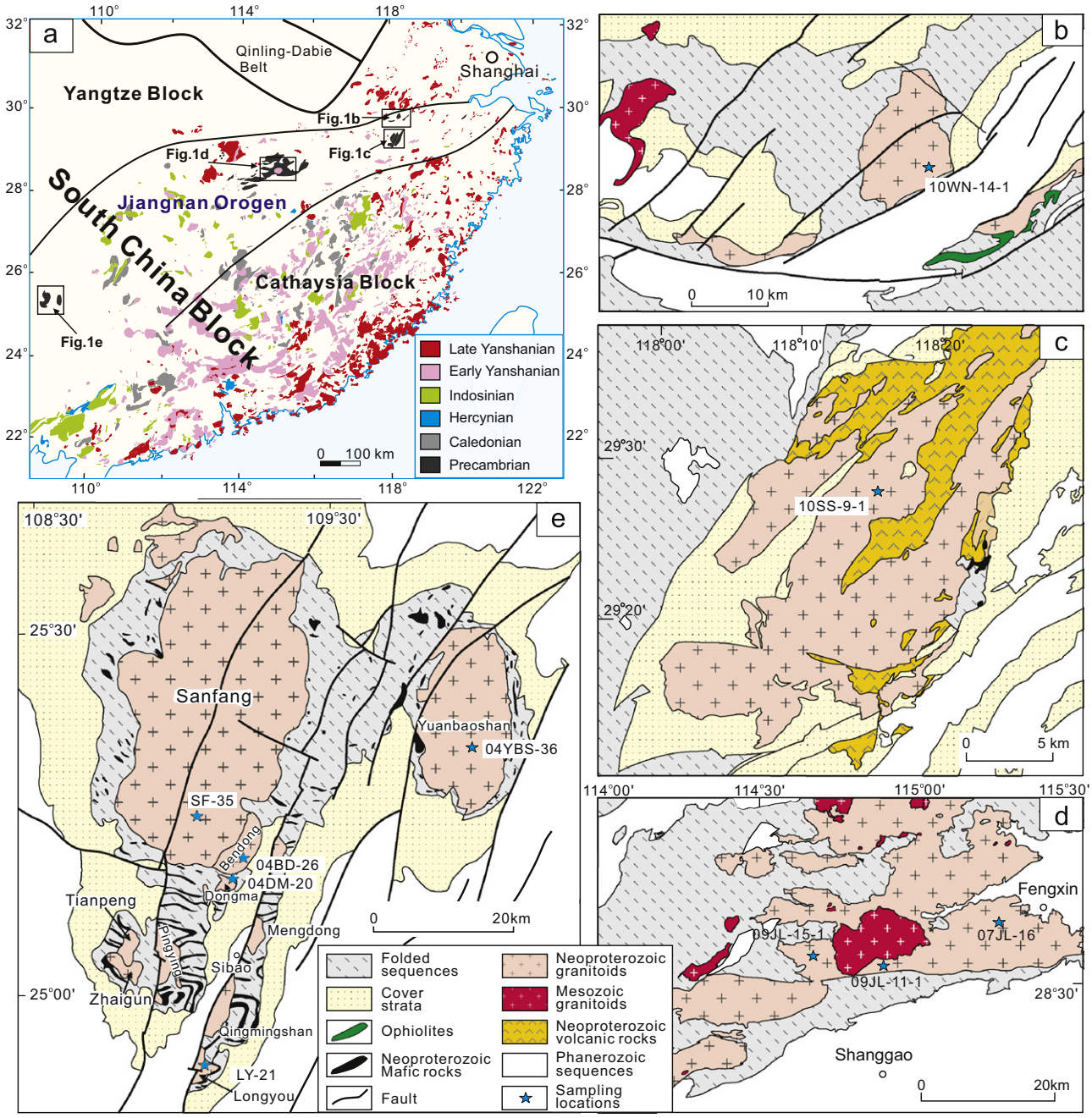

Fig. 1. (a) Geological map of southern China showing the Neoproterozoic granitoids (black) in the Jiangnan orogen. The granitoids of different episodes in the South China Block are indicated with different colors. The studied granitic plutons are shown in: (b) Xucun Pluton, (c) Shi'ershan Pluton, (d) Jiuling Pluton, and (e) northern Guangxi Province (including the Sanfang, Bendong, Yuanbaoshan, Longyou and Dongma plutons). (For interpretation of the references to color in this figure legend, the reader is referred to the web version of this article.)

(NJU). Detailed analytical procedures are given in the Electronic Supplementary Material and the analytical results are listed in Table S1. Mass fractionation of Nd isotopes was corrected by normalizing to $^{146}Nd/^{144}Nd=0.7219$. The $\varepsilon Nd(t)$ values were calculated based on the chondritic uniform reservoir (CHUR) with present-day values of $^{143}Nd/^{144}Nd=0.512638$ and $^{147}Sm/^{144}Nd=0.1967$.

Zircon grains were separated using conventional heavy liquid and magnetic techniques, cast in epoxy, and polished to their mid-section. *In situ* isotope analyses were carried out guided by scanning electron microscopy (SEM) images: secondary electron (SE), back scattered electron (BSE) and cathodoluminescence (CL). Representative CL images are shown in Fig. 2. Zircons were first dated by ion microprobe (SHRIMP U–Pb isotopic analyses, CAGS-Beijing; Table S2). Since many *in situ* U–Pb isotopic data have been published for the granitoids in the JO (*e.g.*, X.H. Li et al., 2003; Z.X. Li et al., 2003Wang et al., 2006; Wu et al., 2006), this work was mainly aimed at determining the variability of ages in zircons that show complex textures (*e.g.*, cores and rims) in CL images. Some zircons were dated by LA-ICP-MS (213 nm New Wave laser system attached to an Agilent 7500a, MiDeR-NJU, Nanjing; Table S2) after O isotope analyses. Oxygen isotope ratios (Table S3) were analyzed in the dated portions of the same zircons using a CAMECA IMS-1280 ion microprobe (WiscSIMS, UW-Madison) after removal of the SHRIMP U–Pb pits. Most $\delta^{18}O$ measurements are from Neoproterozoic magmatic zircon cores (referred to as 'zircon core') or overgrowths on magmatic cores

Table 1
A summary of Neoproterozoic granitic pluton and sample locations in the Jiangnan Orogen.

Pluton	Location	Size	Sample	Rock type	Latitude, Longitude	Age (Ma)	SiO_2 (wt%)	ASI	Zr (ppm)	εNd(t) (WR)
Eastern JO										
Jiuling	NW Jiangxi Province	3860 km^2	09JL-11-1	Granite	N28°33′24″, E114°51′36″	819 ± 9	69.40	1.20	191	−1.30
			09JL-15-1	Granodiorite	N28°33′30″, E114°41′53″		69.17	1.61	186	−3.22
			07JL-16	Diorite enclave	N28°39′24″, E115°17′19″		61.50	1.18	200	−2.20
Xucun	S Anhui Province	130 km^2	10WN-14-1	Granodiorite	N29°55′59″, E118°23′33″	823 ± 8	63.71	1.33	283	−1.08
Shi'ershan	S Anhui Province	500 km^2	10SS-9-1	Granite	N29°28′39″, E118°14′01″	779 ± 11	76.44	1.08	152	−0.99
Western JO										
Bendong	N Guangxi Province	40 km^2	04BD-26	Granodiorite	N25°10′3″, E108°49′22″	823 ± 4	70.28	1.27	245	−5.00
Dongma	N Guangxi Province	4 km^2	04DM-20	Granodiorite	N25°08′39″, E108°49′37″	824 ± 13	60.84	1.80	175	−5.44
Yuanbao-shan	N Guangxi Province	300 km^2	04YBS-36	Granite	N25°17′17″, E109°11′55″	824 ± 4	72.53	1.48	173	−5.57
Sanfang	N Guangxi Province	1000 km^2	SF-35	Granite	N25°15′24″, E109°3′20″	804 ± 5	76.94	1.17	162	−5.85
Longyou	N Guangxi Province	8 km^2	LY-21	Granodiorite	N24°45′20″, E109°4′10″	832 ± 5	65.00	1.15	185	−5.30

Note: ASI, aluminum saturation index. Sources of age data include: Li (1999), X.H. Li et al. (2003), Z.X. Li et al. (2003), Wang et al. (2006) and Wang et al. (submitted for publication). Analyses for the whole-rock SiO_2 and εNd(t) are from this study and Wang et al. (2006). WR—whole rock.

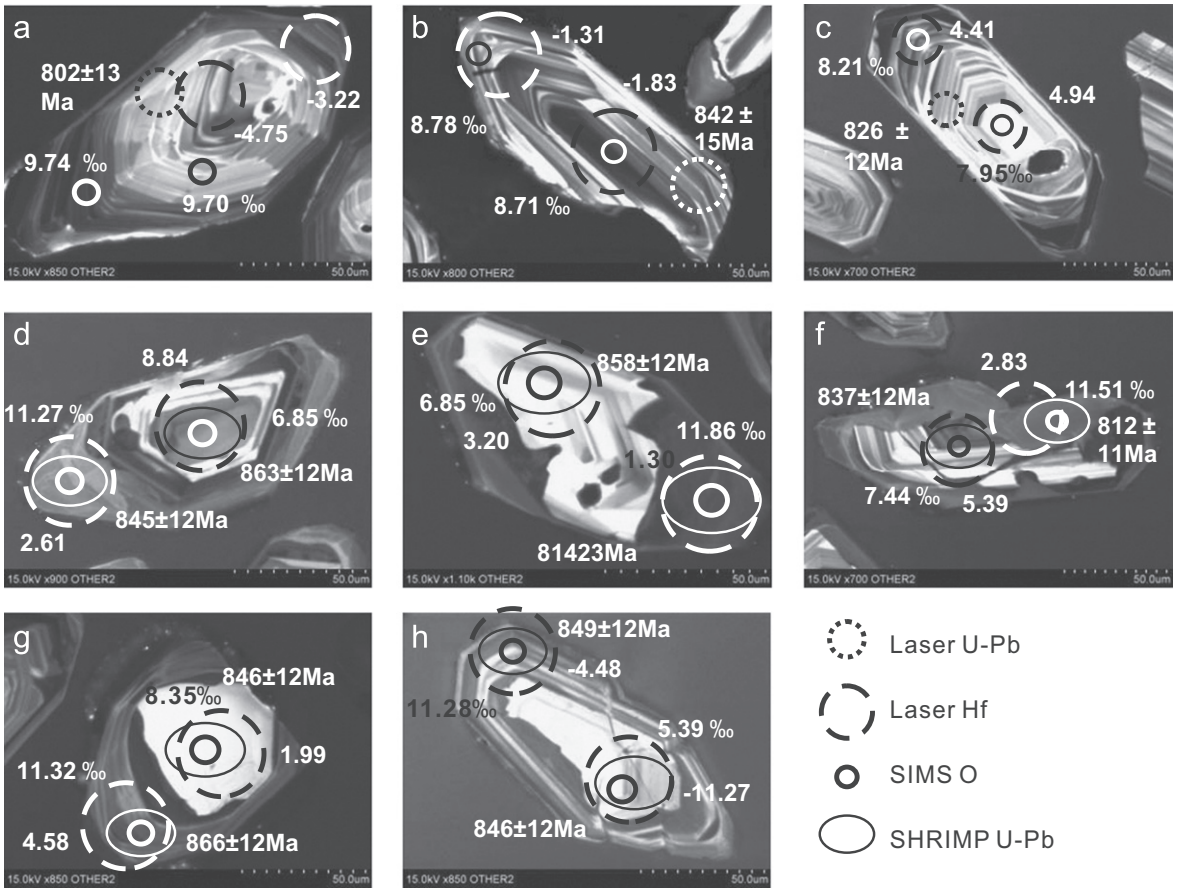

Fig. 2. Representative cathodoluminescence (CL) images of zircon from the Jiangnan orogen (JO). (a)–(b), from the western JO. (c)–(h), from the eastern JO. (a), Bendong Pluton; (b), Dongma Pluton; (c), 09JL-11-1 from the Jiuling Pluton; (d)–(f), 09JL-15-1 from the Jiuling Pluton; (g)–(h), 10WN-14-1 from the Xucun Pluton. (d)–(h) show the zircons with clearly defined cores. The analysis pits and results of SIMS O and U–Pb and laser U–Pb and Hf are indicated.

(referred to 'zircon rim') of individual zircons. A few older inherited cores (2700–860 Ma) were also identified by SHRIMP before oxygen isotope analyses. Finally, Hf isotopes (Table S4) were determined in the same zircon domains using a New Wave ArF 193 nm laser ablation system attached to a Neptune (Plus) MC-ICP-MS (MiDeR-NJU, Nanjing). Whole-rock oxygen isotope ratios of folded metasedimentary units (granitoid wallrock) (Table S5) were analyzed in an airlock sample chamber by laser fluorination and gas-source mass spectrometer at the UW-Madison (Valley et al., 1995; Spicuzza et al., 1998).

4. Results

4.1. Zircon U–Pb dating

In situ analyses yield largely concordant U–Pb system, despite high U contents (900–1580 ppm, Table S2) in some grains. Most zircons give mean ages identical to those listed in Table 1. Note zircons of samples 10WN-14-1 (Xucun Pluton) and 09JL-15-1 (Jiuling Pluton) typically show clearly defined cores in CL (Fig. 2 and Fig. DR1), but U–Pb ages from the cores and rims of these

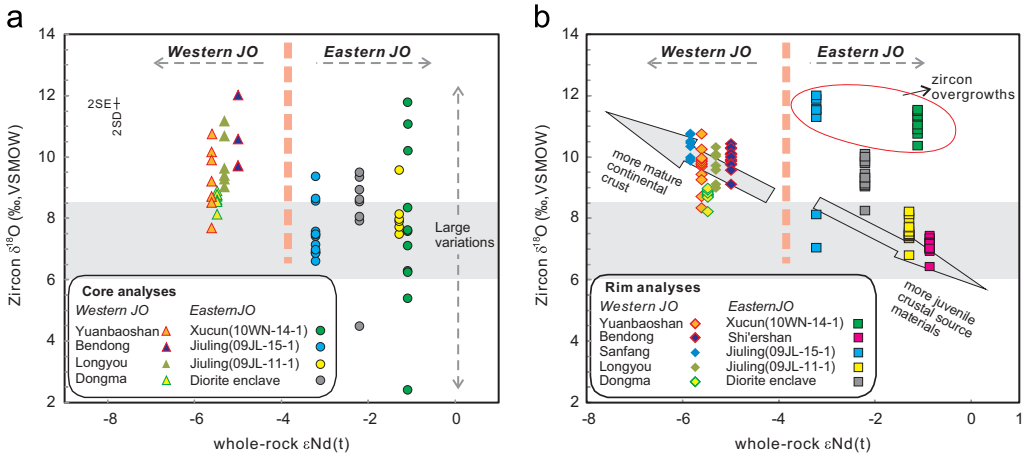

Fig. 3. Zircon $\delta^{18}O$ *versus* whole-rock εNd(t) diagram for the Neoproterozoic granitoids in the Jiangnan orogen (JO). εNd(t) is calculated based on their mean U–Pb ages. The analyses from zircon cores (A) and rims as well as overgrowths (B) are shown separately. The shaded area shows the range of 6.0–8.5‰ in zircon $\delta^{18}O$.

grains are generally the same within analytical uncertainties and identical to the crystallization ages of the two samples (Table S2). For example, the cores and rims of 09JL-15-1 zircons yield consistent mean $^{206}Pb/^{238}U$ ages of 838 ± 11 Ma and 831 ± 21 Ma, respectively. Nonetheless, the analyses differ in that rims generally have Th contents (<50 ppm) and Th/U ratios (<0.15) (Table S2) that are lower than typical values (Th/U >0.3; Vavra et al., 1999) for magmatic zircons.

Three *in situ* U–Pb SHRIMP analyses were carried out on the same zircon grain 04YBS-36♯15 (Yuanbaoshan Pluton), and two of them show slight discordance, even though the three $\delta^{18}O$ analyses corresponding to these ages are identical (Fig. DR1i). One analysis (LY-21♯15) from the Longyou Pluton yield a discordant (mixed) age resulting from overlap of the core–rim boundary by the analysis pit (Fig. DR1i). In addition, one zircon core analysis (JL16♯19c) from the diorite enclave of the Jiuling Pluton shows a $^{207}Pb/^{206}Pb$ age of *ca.* 2.4 Ga (Table S2).

4.2. Zircon O isotopes

Zircon oxygen isotope ratios vary from pluton to pluton, from grain to grain within a single sample, and within individual zircon grains. Two plutons (Sanfang and Dongma) from the western JO and one pluton (Shi'ershan) from the eastern JO have approximately homogeneous $\delta^{18}O$ values in magmatic zircons (Fig. 3a,b; Table S3), with average values of 10.3 ± 0.7‰ (2SD, $n=8$), 8.7 ± 0.5‰ (2SD, $n=16$) and 7.1 ± 0.5‰ (2SD, $n=15$), respectively. Zircon $\delta^{18}O$ values from the Bendong Pluton in the western JO are homogeneous except for one outlier analysis. Similarly, zircon $\delta^{18}O$ values from sample 09JL-11-1 of the Jiuling Pluton from the eastern JO are homogeneous except for one outlier analysis (Fig. 3; Table S3).

Zircons lacking distinct core and rim domains have essentially homogeneous $\delta^{18}O$ values, with core/rim ($\Delta^{18}O_{rim-core}$) of −1.0‰ to 1.0‰ (Fig. 5a) averaging at 0.05 ± 0.68 (2SD); however, zircons with textually distinct cores show considerable intragrain $\delta^{18}O$ variability. The largest intragrain variations in $\delta^{18}O$ values occur in zircons with clearly defined cores from samples 10WN-14-1 (Xucun Pluton) and 09JL-15-1 (Jiuling Pluton). The large $\delta^{18}O$ variation of sample 09JL-15-1 reflects a few rim analyses that are higher than 10‰ (Fig. 3a,b). The bulk of the core analyses for 09JL-15-1 are concentrated within the range of 6.5–7.5‰, except three outliers (Fig. 3a). Two 09JL-15-1 zircons that lack clearly defined cores (Fig. 3b) give outlier rim analyses (Fig. DR1b) that resemble the core analyses of this sample. These two zircons may have formed at the same time as zircon cores and earlier than

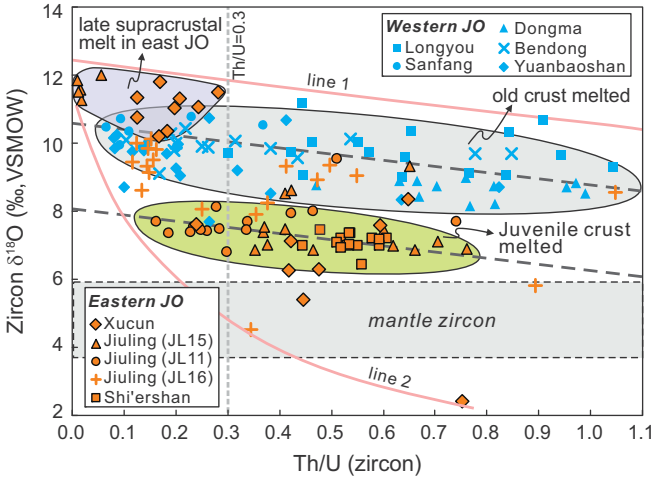

Fig. 4. $\delta^{18}O$ *versus* Th/U plot for zircons in the Jiangnan orogen (JO). All analyses are plotted within the area with two boundaries defined as line 1 ($\delta^{18}O = -1.8 \times (Th/U) + 12.5$) and line 2 ($\delta^{18}O = -2.24 \times \ln(Th/U) + 1.95$). The analyses from the eastern JO constitute two populations. One is characterized by high $\delta^{18}O$ (>10‰) and low Th/U (<0.3). The other defines a rough negative correlation paralleling (with an approximate slope of -1.8) to the trend of analyses from the western JO.

high-$\delta^{18}O$ zircon rims. If the two outlier rim values are grouped with the core analyses of sample 09JL-15-1, their average $\delta^{18}O$ value is consistent with $\delta^{18}O$ values in the other Jiuling Pluton sample (09JL-11-1). Interestingly, one outlier core analysis from 09JL-11-1 gives a $\delta^{18}O$ value essentially identical to highest $\delta^{18}O$ core analysis in samples 09JL-15-1 and 07JL-16 from the same Jiuling Pluton (Fig. 3a,b). Core analyses of sample 10WN-14-1 show the largest $\delta^{18}O$ variation, but the rim $\delta^{18}O$ values in this sample are homogenous. Many analyses from the eastern JO have high $\delta^{18}O$ but low Th/U ratios of <0.3 (Fig. 4).

A few zircons in the diorite enclave (07JL-16) of the Jiuling Pluton show clearly defined cores with $\delta^{18}O$ similar to samples 10WN-14-1 and 09JL-15-1 (Fig. DR1e). One unusual grain (JL16-02♯) has a core $\delta^{18}O$ of 4.5‰ and rim $\delta^{18}O$ of 9.1‰ (Fig. 5a; Table S3).

4.3. Zircon Hf isotopes

There is a larger data set of Hf isotopes than that of oxygen isotopes for the Neoproterozoic zircons. Broadly, εHf(t) values are predominantly negative in the western JO but positive in the eastern JO, consistent with the contrasting whole-rock Nd

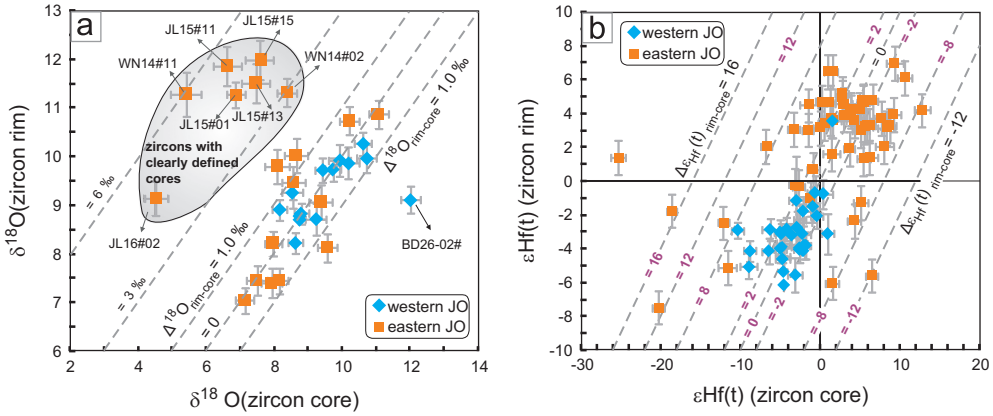

Fig. 5. The variations of $\delta^{18}O$ and εHf(t) in individual zircons of the Neoproterozoic granitoids in the Jiangnan orogen (JO). Zircon grains that have only one analyzing pit are not plotted. Fig. 3A shows that most grains have no significant core–rim variations in $\delta^{18}O$ ($\pm$ 1‰) except those with clearly defined cores. Fig. 3B indicates that the Hf isotopes vary greatly across some zircons, especially in the eastern JO. Analytical precision is plotted as 2SE for εHf and 2SD for $\delta^{18}O$.

isotopes of the eastern and western JO (Fig. 6). A few analyses in the eastern JO have negative εHf(t) (Fig. 5b).

Hf isotope compositions are nearly identical across western JO zircons that lack distinct cores and rims, whereas some zircons with clearly defined cores from the eastern JO show significant variations (Fig. 5b). Within samples, rim values of εHf(t) are homogeneous from grain to grain, regardless of variation in the cores (Fig. 7a). Similarly, $\delta^{18}O$ tends to be homogenous among zircon rims (Fig. 7b).

5. Discussion

5.1. Covariations of Th/U and $\delta^{18}O$ in zircon

JO zircon data define two parallel negative trends on a plot of Th/U *versus* $\delta^{18}O$ (Fig. 4). The lower trend is defined by core analyses from zircons with distinct cores and zircons lacking clearly defined cores in the eastern JO, whereas the uppermost trend is defined almost exclusively by analyses from the western JO. These systematic negative trends are not consistent with a shift in magma source rocks, which would be expected to produce significant scatter in Th/U *versus* $\delta^{18}O$.

Th and U substitute for Zr^{4+} in the zircon lattice (Hoskin and Schaltegger, 2003), and Th/U of zircons from silicate magmatic rocks commonly range from 0.1 to 1.0 (Belousova et al., 2002). Factors that affect Th/U in zircons include: source rock composition, magma composition, temperature, fluids and contemporaneous crystallization of other Th- and/or U-enriched minerals.

Magma source rocks are a primary control on granitic magma chemistry (Clemens and Stevens, 2012) and thus likely exert strong control on Th/U in zircons. For example, magmatic zircons from the Tertiary igneous rocks of the Mojave terrane have typically high Th/U (*ca.* 1–4.5) that reflect interactions between magmas and the Proterozoic Mojave lithosphere (Claiborne et al., 2010). Calculations from experimental studies corroborate empirical studies showing that Th/U in igneous zircons is usually positively correlated with magma temperature (Claiborne et al., 2010; Barth and Wooden, 2010). Moreover, partitioning and preferential removal of highly compatible U by oxidizing fluids will enrich magma in Th and may significantly increase Th/U in crystallizing zircons. Conversely, the enrichment of fluids in the later stage of granitoid magmatic evolution will result in high Th/U in mineral phases (including zircon). Finally, it is difficult to relate intragrain Th/U variations in zircon to crystallization of Th- and/or U-enriched minerals (monazite, thorite, *etc.*) without exhaustive texturally analysis and geochronology.

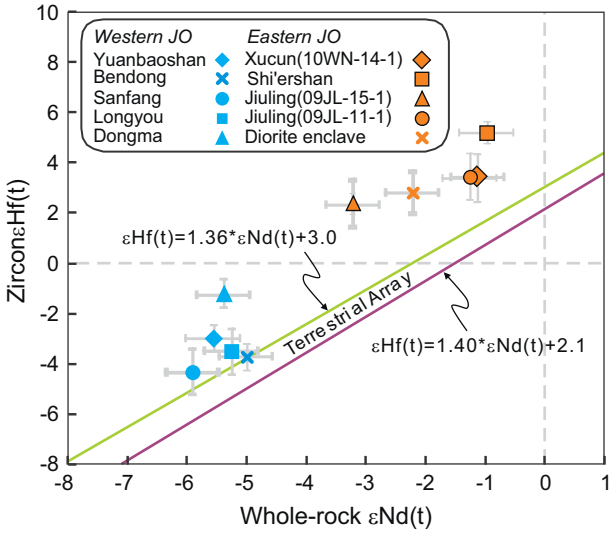

Fig. 6. Zircon εHf(t) *versus* whole-rock εNd(t) for the Neoproterozoic granitoids in the Jiangnan orogen (JO). εHf(t) and εNd(t) are calculated based on the U–Pb ages for different plutons. Two equations of Nd–Hf isotopes and the terrestrial array are from Vervoort and Blichert-Toft (1999).

Kemp et al. (2007) related decreasing Th/U ratios in zircons from the Lachlan Fold Belt to magmatic differentiation and associated magmatic cooling. We suggest that the negative Th/U–$\delta^{18}O$ correlations of the JO (Fig. 4) are the result of a combination of AFC (crustal assimilation and magmatic fractional crystallization) processes and late-magmatic fluids. AFC processes, including assimilation of weathered supracrustal wallrock, should simultaneously increase $\delta^{18}O$ and drive down Th/U by cooling the magmas. In addition, fluids were enriched in the late-stage magmas, as evidenced by the widespread occurrence of tourmaline in granites of the western JO. Such fluids may have increased magmatic $\delta^{18}O$, especially in the western JO. The subset of zircons from the eastern JO following that define the lower Th/U–$\delta^{18}O$ trend may have formed by this mechanism, although this lower trend shows a narrower range of Th/U (Fig. 4) and may indicate limited magmatic differentiation.

5.2. Formation of the high-$\delta^{18}O$ zircon rims in the eastern JO

In addition to the two trends discussed above, rim analyses of zircons with clearly defined cores cluster in the top left corner of the Th/U–$\delta^{18}O$ plot (Fig. 4). The analyses within this cluster are

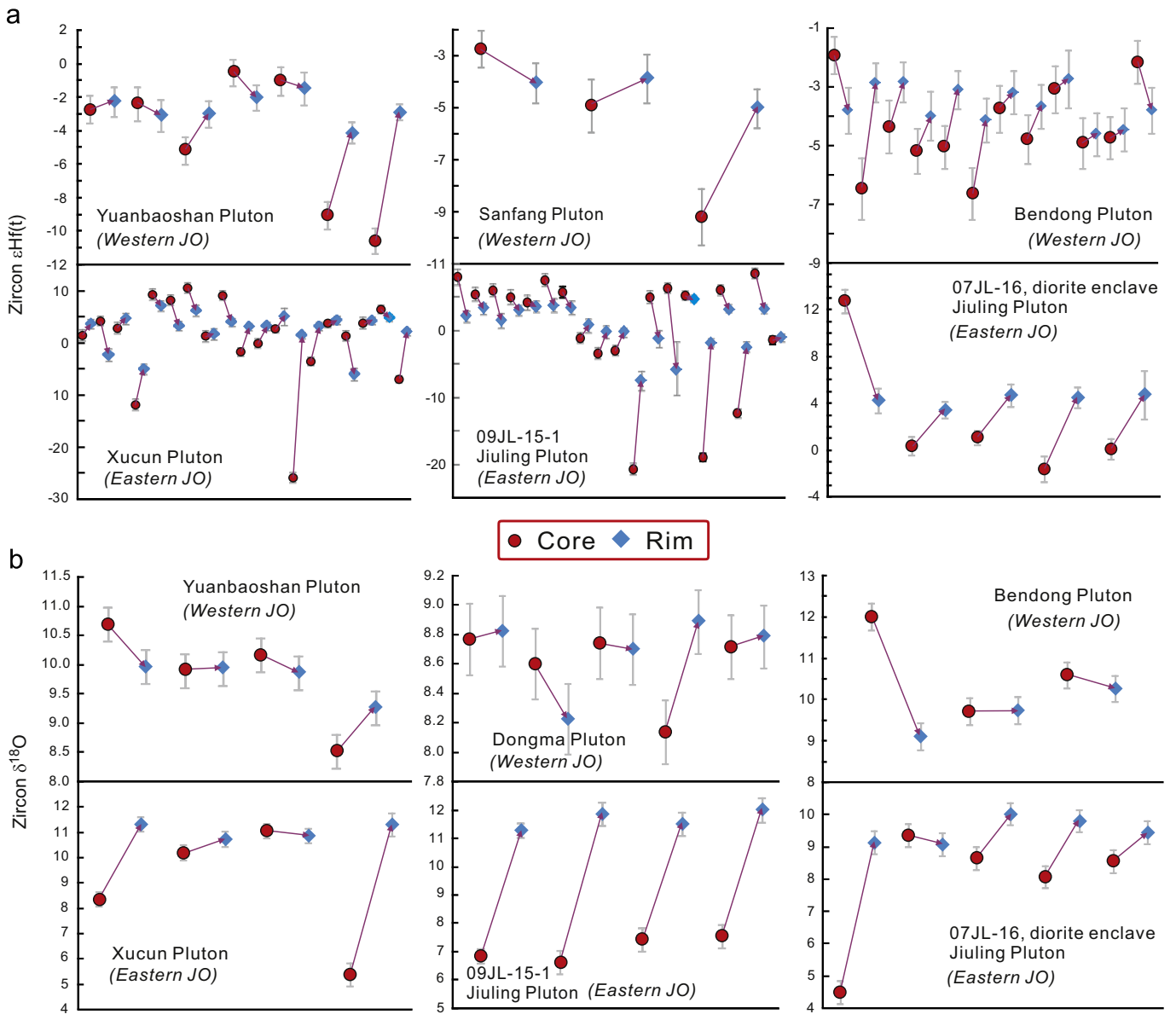

Fig. 7. Variations of εHf(t) and $\delta^{18}O$ in individual zircons for different plutons in the Jiangnan orogen (JO). The red circles and blue diamonds represent the analyses from cores and rims respectively. (For interpretation of the references to color in this figure legend, the reader is referred to the web version of this article.)

from the zircons of the Xucun (10WN-14-1) and Jiuling (09JL-15-1) Plutons and partially overlap the upper negative trend defined by the analyses from the western JO (Fig. 4).

High-$\delta^{18}O$ zircon rims could be either metamorphic or magmatic in origin. High-temperature, high-$\delta^{18}O$ metamorphic fluids can precipitate high-$\delta^{18}O$ zircon overgrowths. For example, high-$\delta^{18}O$ zircon overgrowths in paragneiss of the Kapuskasing Uplift (Canada) formed from granulite-facies metamorphism and show core–rim oxygen isotope variations similar to those described here for the JO (Bowman et al., 2011). However, there is no evidence for high-grade regional metamorphism or anatexis of the country rocks surrounding the Neoproterozoic JO granitoids (X.H. Li et al., 2003; Wu et al., 2006; Wang et al., 2007). Moreover, zircons could retain their initial Hf isotopic composition even through high-grade metamorphic recrystallization (Zheng et al., 2005). Thus, the distinct differences in εHf(t) between eastern JO zircon cores and rims (Fig. 7a) are most consistent with rim formation by a later phase of magmatic crystallization.

In this study, ~97% of zircon grains (354 of 364) from 09JL-15-1 (Jiuling Pluton) and ~53% of zircons (155 of 293) from 10WN-14-1 (Xucun Pluton) have clearly defined cores (Fig. 2). The sharp, irregular core–rim boundaries suggest that low Th/U, high-$\delta^{18}O$ rims of eastern JO zircons grew from magmatic melts and/or fluids. The widespread occurrence of rim overgrowths would require voluminous and pervasive magmatic fluids for which there is no field or petrographic evidence: neither the mineral assemblage, nor the degree of alteration changes significantly across a given pluton. We therefore infer that eastern JO core–rim morphologies record rim growth from a different magma composition. We believe that lower Th/U and elevated $\delta^{18}O$ reflect input of supracrustal materials during the evolution of eastern JO magmas. Zircons that plot in the top-left cluster in Fig. 4 but do not show clearly defined cores (Fig. DR1d) likely crystallized directly from the late-stage high-$\delta^{18}O$ magmas.

5.3. Genesis of the clearly defined cores in the eastern JO

U–Pb ages are permissive of two possible interpretations for the eastern JO zircon cores—(1) core inheritance from a slightly earlier ($\leq$ 30 Myr) but petrogenetically unrelated magmatic cycle,

or (2) crystallization and partial resorption during an extended 860–820 Ma magmatic cycle. Several lines of evidence indicate that eastern JO zircon cores crystallized during an extended Neoproterozoic magmatic cycle and are geochemically related to their high-$\delta^{18}O$ rims.

Samples with clearly defined zircon cores generally show high whole-rock Zr concentrations (*ca.* 185–280 ppm; Table 1) and correspondingly high Zr saturation temperature (829 ± 18 °C; Wu et al., 2006), consistent with the inheritance-poor granitoids (mean of 837 ± 48 °C) compiled by Miller et al. (2003). However, the proportion of zircons with clearly defined cores in eastern JO samples (53% and 97%, see above) is more consistent with zircon persistence in an evolving magma than zircon inheritance. If inherited zircons had survived high temperature (>800 °C) partial melting (Clemens, 2003), the newly-crystallized zircon rims should have normal Th/U, instead of the observed low Th/U ratios (<0.3; Fig. 4). Some eastern JO samples do not have clearly defined cores (this study and our unpublished data). For example, rare zircon cores were found in zircons of 09JL-11-1 (Fig. DR1a) like those in 09JL-15-1, although the two samples have similar whole-rock geochemical compositions (*e.g.*, SiO_2 and Zr contents; Table 1). Furthermore, zircons from the most likely potential source of 'inherited' Neoproterozoic cores, 860–830 Ma diorites exposed along the Jiangshan–Shaoxing Fault in the arc–continent collisional belt, show low zircon $\delta^{18}O$ values (*ca.* 5‰; unpublished data) that are inconsistent with eastern JO core $\delta^{18}O$ values.

Finally, the interpretation that zircon cores formed during the early stage of the same magmatic cycle is supported by the oxygen isotopes in zircons from the Jiuling Pluton. Excluding high-$\delta^{18}O$ (>10‰) rims, all zircon analyses (cores and two rims) for sample 09JL-15-1 fall in the range 6.9–9.3‰, with a mean value of 7.5 ± 0.4‰ (2SD, $n=15$). This mean $\delta^{18}O$ is similar to the $\delta^{18}O$ values (mean of 7.8 ± 1.1‰, 2SD; with one outlier; Fig. 3a) of another Jiuling Pluton sample (09JL-11-1) in which zircons do not have clearly defined cores. This suggests a shared source for both 09JL-15-1 and 09JL-11-1 and a shared magma chamber in which oxygen isotope system equilibrated and largely homogenized in the early stage of melting. One outlier core analysis of 9.5‰ from 09JL-11-1 probably indicates minor source heterogeneity.

The other eastern JO sample with clearly defined cores (10WN-14-1) shows the largest core $\delta^{18}O$ variations. Some of the cores may be inherited from rocks or weathered remnants of an earlier magmatic cycle. An alternative explanation is that theses cores indicate greater heterogeneity in early-stage melts of the Xucun Pluton than in early-stage melts of the Jiuling Pluton. The mean core $\delta^{18}O$ value from sample 10WN-14-1 falls within the range (6.0–8.5‰) of eastern JO zircons without defined cores (Fig. 3a, b). We therefore infer that the overall oxygen isotope compositions of the sources of the early-stage magmas for sample 10WN-14-1 are the same as for other Neoproterozoic granitoids in the eastern JO.

5.4. Petrogenesis of the Neoproterozoic granitoids in the JO

As discussed above, the cores represent the early melt within the same magmatic cycle (*i.e.* one evolving magma), while the rims record the final melt. We discuss the details of JO granitic magmas at the early and later stages below.

In the early stage of magmatic evolution, zircon cores should reflect the geochemical characteristics of the magma source. Large variations of oxygen and hafnium isotope ratios within the cores may indicate melting of heterogeneous source rocks. Isotopic variability related to heterogeneous source rocks will be enhanced by rapid extraction of melt in batches. Source heterogeneity and batch melting would not affect the U–Pb ages of zircons forming at the early stage.

The high $\delta^{18}O$ rims of eastern JO zircons require voluminous melting and assimilation of high-$\delta^{18}O$ source rocks. Wu et al. (2006) reported the oxygen isotope ratios of bulk zircon mineral separates measured by laser fluorination for the Xucun Pluton with $\delta^{18}O$ at 8.1–10.1‰, mostly concentrating at 9.0–9.8‰, which represents the mixing of defined cores and rims. Mass balance considerations indicate assimilation and/or mixing of at least 50% supracrustal melts into the existing magma to generate these mixed $\delta^{18}O$ values. If the folded metasedimentary wallrocks of the eastern JO are considered to be one endmember, mixing models based on zircon oxygen and Hf isotopes (Fig. 8) indicate over 60% wallrock contribution for the late-stage Xucun magma and over 85% contribution for the late-stage Jiuling magma (Fig. 8). It is energetically impossible to incorporate such a high percentage of wallrock by assimilation. Therefore, voluminous supracrustal melts must have been injected into a deeper magma chamber before the magma intruded its final position. Late-stage anatexis of supracrustal rocks suggests a heat contribution from mantle in the form of basaltic underplating.

In contrast, zircon core–rim $\delta^{18}O$ variations in the Neoproterozoic granitoids of the western JO are neither as large nor as consistent as $\delta^{18}O$ variations in eastern JO granitoids (Figs. 3 and 5; Table S3), suggesting that their magmatic evolution did not involve mixing of distinctly different sources with different sources with different $\delta^{18}O$ values. Instead, the consistently higher $\delta^{18}O$ values (generally >8.5‰) of western JO zircon cores and rims (Fig. 3) imply magma contributions predominantly from supracrustal materials. Although the analyses in the western JO fall on a single mixing curve of two end-members, individual samples have more restricted Hf–O isotope values (Fig. 8), indicating that their magmatic evolution was not as complicated as in the eastern JO.

All Neoproterozoic JO granitoids show different degrees of isotopic heterogeneity at different times in their magmatic evolution as evidenced by greater core-to-core than rim-to-rim isotopic variability (Fig. 7). Rim Hf and oxygen isotope values are more homogenous than core analyses, suggesting that the strongly peraluminous granitic magmas generally reach the Hf–O isotope homogeneity in the later stages of magmatic evolution, and that rim analyses may be the best estimation for the isotope compositions of the final homogenized magma.

Zircons from a diorite enclave (07JL-16) in the eastern JO Jiuling Pluton show a large range of Th/U, similar to zircons of the western JO, and widely varying $\delta^{18}O$ values. Some of the enclave zircon analyses are similar to the eastern JO analyses, but the majority plot along the negative trend defined by western JO zircons in the Th/U–$\delta^{18}O$ diagram (Fig. 4). One enclave zircon (07JL-16#02) also has a clearly defined core (Fig. DR1e). Hf (Fig. 7a) and O (Fig. 7b) isotopes are more homogeneous from rim-to-rim than from core-to-core in zircons from this diorite enclave. The enclave core analyses plot between the western and eastern JO on mixing Line-A of the $\varepsilon Hf(t)$–$\delta^{18}O$ diagram (Fig. 8), whereas enclave rim analyses plot between eastern JO rim and core analyses from zircons with clearly defined cores (*i.e.* Line-B and C; Fig. 8). Therefore, the diorite enclave records late mixing of high-$\delta^{18}O$ supracrustal melt, similar to other eastern JO samples, and does not represent injection of depleted mantle-derived magmas into the granitic Jiuling magmas.

5.5. Implications for the genesis of "S-type" granitoids

The previous work on *ca.* 820 Ma eastern JO granitoids showed an apparent decoupling between their isotopic and major element compositions (*e.g.*, Zhou and Wang, 1988). Positive zircon $\varepsilon Hf(t)$ and low-negative whole-rock $\varepsilon Nd(t)$ are consistent with typical I-type granitoids, whereas occurrences of garnet and

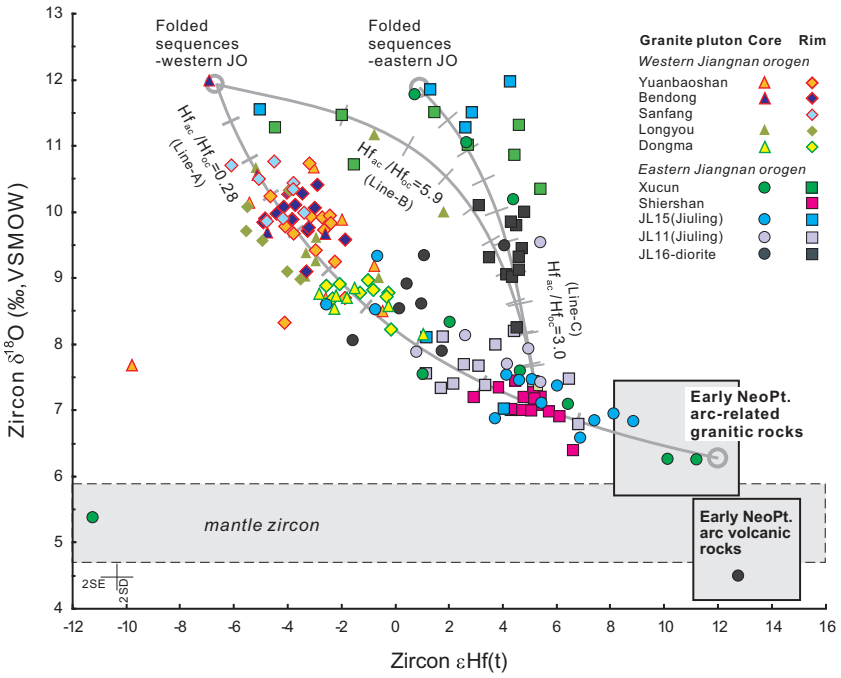

Fig. 8. $\delta^{18}O$–εHf(t) diagram for magmatic zircons of the Neoproterozoic granitoids in the JO, showing calculated curves for mixing in the sources. Different proportions of arc and mature continental crust lead to specific Hf–O isotopic values for different plutons, especially for the western JO. Granitoids from the eastern JO generally have varying oxygen isotopes and high $\delta^{18}O$ rims, indicating large percentages of supracrustal melt. The εHf(t) values for zircons from the arc-related granitic and volcanic rocks are calculated at their U–Pb ages (900–915 Ma; Ye et al., 2007; Li et al., 2009), and their bulk $\delta^{18}O$ values are from Qi et al. (1986) and Ye (2006). Two supracrustal end-members are indicated by open circles: mature continental crust (folded metasedimentary sequences) of western JO with $\delta^{18}O$=11.9‰ and εHf(820 Ma)= −6.7, and folded metasedimentary sequences of eastern JO with $\delta^{18}O$=11.9‰ and εHf(820 Ma)=0.9. These two crustal endmembers are mean values of samples from the folded metasedimentary sequences in the western and eastern segments of the JO, respectively. The values of εHf(820 Ma) of the folded metasedimentary sequences are calculated from their whole-rock εNd(820 Ma) values of fresh samples by the equation of Vervoort and Blichert-Toft (1999). The $\delta^{18}O$ values of metasediments from the folded sequences are reported in Table S3. Error bars depict the average 2SE uncertainty for Hf and 2SD for $\delta^{18}O$. Ticks on the curves represent 10% mixing increments. The ratio of Hf concentrations in the arc crust (ac) and old crust (oc) end members (Hf_{ac}/Hf_{oc}) is indicated for each mixing line.

cordierite in associate with high ASI are consistent with typical S-type granitoids. The *in situ* Hf–O isotope studies of zircons reveal complex magmatic processes for these granitoids. The early-stage magmas formed granitoids like 09JL-11-1, lacking garnet and cordierite, whereas the late-stage magmas generated granitoids like 09JL-15-1 and 10WN-14-1, with abundant garnet and cordierite. Especially, the early-stage magma shows $\delta^{18}O$(zircon) values mainly at 6.0–8.5‰, while the late melt shows $\delta^{18}O$(zircon) at 10.5–12.5‰ (Fig. 3a,b). Recently, Kemp et al. (2009) showed that the Caledonian S-type and I-type granites in the Australian Tasmanides have $\delta^{18}O$(zircon) of 8–10‰ and 6–8.5‰ respectively. Thus, the early-stage magmas represented by eastern JO sample 09JL-11-1 are similar in $\delta^{18}O$ to I-type granitoids, while the late-stage melts, represented by samples 09JL-15-1 and 10WN-14-1, resemble S-type granitoids. The change in zircon $\delta^{18}O$ shows that the magmas of S-type granitoids can evolve from I-type-like magmas through variable amounts of crustal assimilation and magma mixing (*e.g.*, Collins, 1996; Zhu et al., 2009). This also offers an explanation for granitoids that show characteristics of both I- and S- type granitoids (Chappell and White, 2001; Clemens, 2003; Ferreira et al., 2003; Zhu et al., 2011).

5.6. Magma source: crustal growth and recycling

Most of the data from the western JO zircons, eastern JO zircons without clearly defined cores, and eastern JO analyses of clearly defined zircon cores fall along a mixing line (Hf_{pm}/Hf_c=0.28; Line-A) between western JO folded metasedimentary rocks and the eastern JO arc-related rocks (Fig. 8). This mixing trend is similar to the mixing trend for granites of the Lachlan Fold belt (Kemp et al., 2007). The juvenile arc crustal component is represented by the early Neoproterozoic (915–900 Ma; Ye et al., 2007; Chen et al., 2009) volcanic rocks and granitoids in the eastern JO whose zircons show Hf isotope compositions comparable to depleted mantle (Chen et al., 2009); however, the dominant mixing trend does not intersect the range of $\delta^{18}O$ values for mantle-like zircons (Fig. 8), and thus the juvenile crustal component must have evolved somewhat beyond pristine mantle-derived rocks.

Isotopic values for JO samples span a wide range of values along the dominant mixing line (Line-A), but within a given pluton, zircon $\delta^{18}O$ and εHf(t) span narrower ranges (2‰ and 4 epsilon units respectively, except in the two samples with clearly defined cores) (Fig. 8). Thus the mixing line is defined by multiple, slightly overlapping compositional ranges, and we infer that it likely reflects differences in initial melt protolith rather than mixing of melt batches from different sources.

The proportions of the evolved continental crust and juvenile arc crust in the sources can be estimated from Fig. 8. The overall proportion of juvenile arc crust decreases significantly from east ($\geq$70%) to west ($\leq$50%) (Fig. 9). These estimates suggest that the Hf isotopic variation between the eastern and western JO granitoids was mainly controlled by the proportion of juvenile arc crust in their sources. The relatively radiogenic Nd–Hf isotope compositions of eastern JO zircons (Fig. 6) do not therefore require direct input of mantle-derived magma into a granitic magma system, although crustal melting was likely caused by intrusion of mantle-derived mafic magma.

Many Neoproterozoic magmatic rocks in the Yangtze Block have late Mesoproterozoic zircon single-stage Hf model ages at *ca.* 1.2 Ga (Wu et al., 2006; Zheng et al., 2008) that are only 300–400 Myr older than their crystallization ages (*ca.* 850–750 Ma).

These late Mesoproterozoic Hf model ages confirm that voluminous juvenile crust was incorporated into sources of the Neoproterozoic magmatic rocks in southern China. In this case, single-stage Hf model ages (T_{Hf1}) are better than crustal model ages (*i.e.*, two-stage model ages, T_{Hf2}) for estimating the timing of juvenile crust growth (*e.g.*, Wu et al., 2006). In contrast to the above-mentioned previous studies in southern China, zircon Hf–O isotopic data for the Neoproterozoic granitoids in the eastern JO suggest mixing between juvenile arc crust and mature continental crust in source rocks, and their zircon single-stage Hf model ages (T_{Hf1}) could not represent definite proxy for the timing of crustal growth.

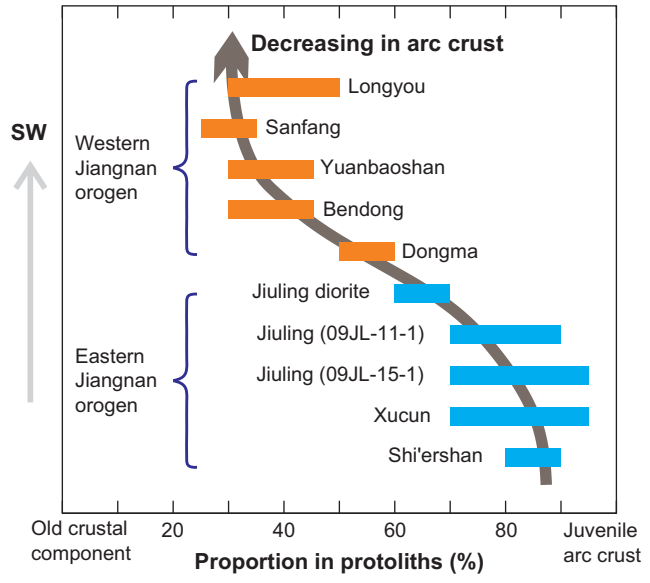

Fig. 9. Range of proportions of mature continental crust and juvenile arc crust in the sources of the Neoproterozoic granitoids in the Jiangnan orogen. The amount of juvenile crust in the sources decreases significantly from the east to west.

We note that different parameters have been used to calculate crustal model age based on the Hf isotope compositions of depleted mantle. For example, both $^{176}Lu/^{177}Hf=0.015$ for present-day bulk continental crust (Rudnick and Gao, 2003; Griffin et al., 2004) and $^{176}Lu/^{177}Hf=0.027$ for mafic crust (Griffin et al., 2004) have been widely used for post-Archean age models. A plot of initial $^{176}Hf/^{177}Hf$ *versus* U–Pb age diagram for JO granitoids (Fig. 10c) shows parallel trends when data are grouped by oxygen isotope composition. The trends are not consistent with model lines calculated using $^{176}Lu/^{177}Hf=0.027$ (Fig. 10b) but do fit model lines calculated with $^{176}Lu/^{177}Hf=0.015$ (Fig. 10a,b,c), suggesting that the bulk continental crust $^{176}Lu/^{177}Hf$ parameter is appropriate for calculating two-stage model ages of Proterozoic and Phanerozoic zircons in southern China. In addition, this average continental value is consistent with whole-rock Lu–Hf isotopic data for the western JO Neoproterozoic metasedimentary cover sequences, which give a mean $^{176}Lu/^{177}Hf$ of 0.0128 ± 0.0026 (2SD, $n=36$) (Wang et al., 2011b).

Fig. 10c shows that $\delta^{18}O$ varies systematically with the initial $^{176}Hf/^{177}Hf$ (Fig. 10c), which is consistent with the results indicated by the Hf–O diagram (Fig. 8). The lowest $\delta^{18}O$ zircons have the highest initial $^{176}Hf/^{177}Hf$, with the exception of one outlier (Fig. 10c). The JO analyses define two parallel arrays (Fig. 10c), with the higher one made up mainly of the eastern JO high-$\delta^{18}O$ analyses and the lower one made up of western JO analyses.

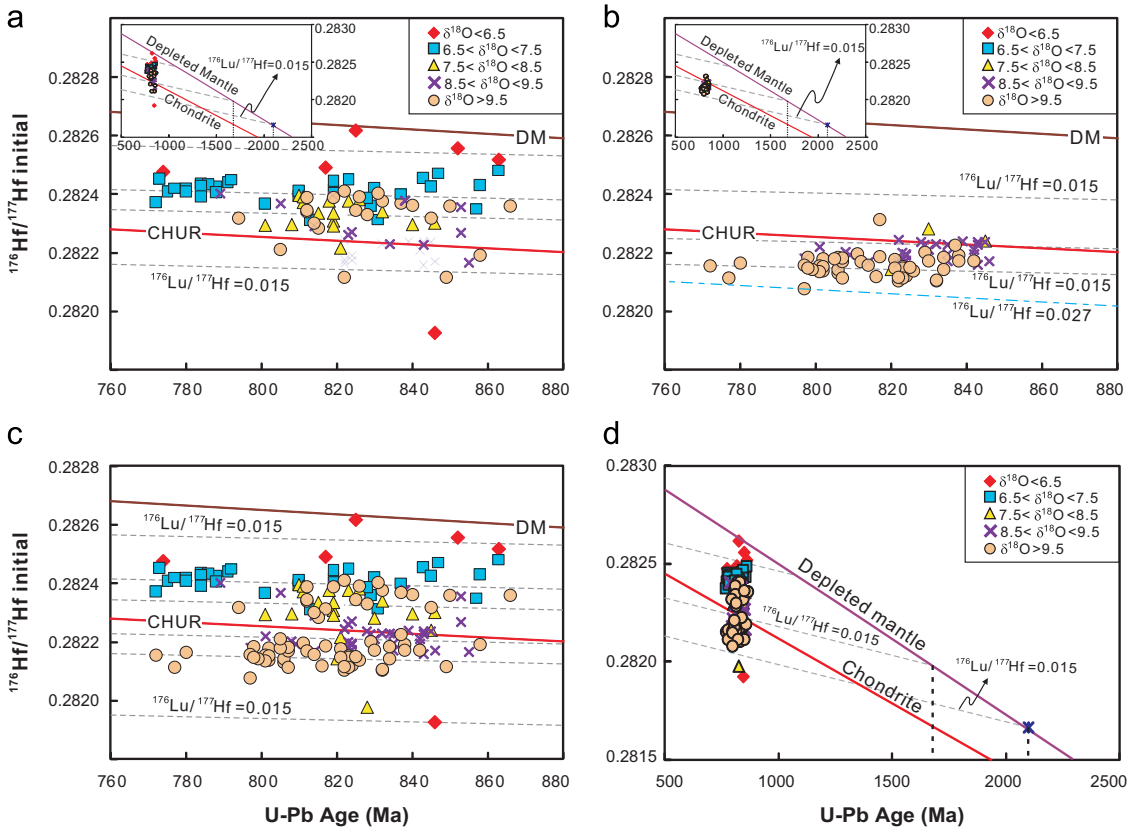

Fig. 10. Initial $^{176}Hf/^{177}Hf$ ratio *versus* U–Pb age diagram for magmatic zircons from the Neoproterozoic granitoids in the Jiangnan orogen (JO). Analyses from the eastern and western JO are shown separately in a and b, and all analyses are shown together in c and d. Values of $\delta^{18}O$(zircon) are shown with different symbols. DM—depleted mantle, CHUR—Chondrite uniform reservoir. The top right inset shows the detailed variations of $\delta^{18}O$ for these analyses.

Eastern JO zircons with $\delta^{18}O$ between 6.5‰ and 7.5‰ show an especially good linear relation, whereas the analyses with $\delta^{18}O > 8.5$‰ show more scatter (Fig. 10a). Western JO zircon T_{Hf2} model ages cluster at 1.7–2.1 Ga (Fig. 10b) and are similar to whole-rock Nd model ages (Table S1), which indicate the reworking of Paleoproterozoic crustal sources. If initial Hf isotope ratios are controlled primarily by magma source as previously discussed, then these coherent, nearly continuous Hf-age trends are consistent with episodic melting of the same source over time and are inconsistent with mixing of granitic and mantle-derived magmas.

5.7. Comparisons with low $\delta^{18}O$ Neoproterozoic magmas of southern China

The Yangtze Block is bounded by multiple Neoproterozoic orogenic/magmatic belts: the Jiangnan orogen to the southeast, the Qinling–Dabie belt to the north, and the Hannan–Panxi belt to the west and northwest. No systematic oxygen isotope data are published for the west and northwestern margins. The Neoproterozoic (*ca.* 820–700 Ma) magmatic rocks along the northeastern margin experienced an ultra-high-pressure (UHP) metamorphism as part of the Triassic Dabie–Sulu metamorphic belt (Fig. 1a; Xu et al., 1992; Li et al., 1993; Ernst et al., 2007). The UHP Triassic metamorphic rocks contain Neoproterozoic zircon xenocrysts and inherited zircon cores (*ca.* 820–700 Ma) with $\delta^{18}O$ lower than mantle zircon and down to –10‰ (Zheng et al., 2004; Chen et al., 2011; Fu et al., in press). Neoproterozoic rifting and the accompanying high-temperature exchange with deeply circulating glacial meltwaters have been proposed to cause the low $\delta^{18}O$ zircon-forming magmas (Zheng et al., 2004). None of the Neoproterozoic JO granitoids (*ca.* 835–780 Ma) have extremely low $\delta^{18}O$. Even the *ca.* 780 Ma Shi'ershan Pluton zircons, which is the same age as protoliths of the UHP rocks in the Dabie–Sulu belt, have $\delta^{18}O$ values of 6.4–7.4‰. We conclude that hydrothermal alteration involving very low $\delta^{18}O$ water did not affected the Neoproterozoic JO granitoids.

Wang et al. (2011a) recently reported data from detrital zircons in the Neoproterozoic (Cryogenian) cover sequences of the western JO. $\delta^{18}O$ values of 0–6‰ (dominantly 5–6‰) and two age peaks at 830–800 Ma and 800–750 Ma suggest a Neoproterozoic igneous provenance with mantle-like oxygen isotope signature for these detrital grains (Wang et al., 2011a). The higher zircon $\delta^{18}O$ values measured in this study rule out the underlying Neoproterozoic JO granitoids as a significant source of sediments for the cover sequences. Detrital zircons also lack negative $\delta^{18}O$ values (Fu et al., in press) and thus it is unlikely that the Dabie–Sulu Neoproterozoic protoliths provided significant sediment to the western JO Neoproterozoic cover sequences. An alternative explanation is that significant uplift and erosion in the western JO removed pre-existing low-$\delta^{18}O$ volcanic rocks that sourced the cover sequences.

6. Conclusions

Combined U–Pb, Hf and O isotope data from zircons show that the deep crustal source rocks for Neoproterozoic strongly peraluminous granitoids of the Jiangnan orogen (JO) vary from east to west. More mature continental crust (generally $>50\%$) was present in the sources for the western JO granitoids, as evidenced by lower hafnium isotope compositions and relatively high oxygen isotope values ($\delta^{18}O$ of 10.5–8.5‰) in zircons. A larger proportion (generally $>70\%$) of juvenile arc crust was incorporated into the sources of eastern JO granitoids, leading to radiogenic hafnium isotopes in zircons. Moreover, it should be noted that this study is really a reconnaissance and that further detailed study might elucidate important petrogenetic details.

Zircons from the eastern JO contain a grain-scale record of granitoid compositional evolution from I-type to S-type. Although all eastern JO granitoids are peraluminous, some are isotopically similar to rocks commonly defined as I-type: they generally lack aluminous minerals (*e.g.*, garnet and cordierite) and have a restricted range of zircon $\delta^{18}O$ values (6.0–8.5‰). Other eastern JO granitoids are mineralogically and isotopically in oxygen similar to rocks commonly defined as S-type: they are enriched in garnet and cordierite and have clearly defined zircon cores surrounded by high-$\delta^{18}O$ rims with similar U–Pb ages. Clearly defined zircon cores formed in melts derived from heterogeneous sources and show large variations in $\delta^{18}O$ and $\varepsilon Hf(t)$. In contrast, zircon rims show a narrow range of elevated $\delta^{18}O$ (12.0–10.5‰), suggesting significant incorporation of partial melts derived from melting of supracrustal rocks at late stage of granite evolution.

Our data show that granitoid classification on the basis of bulk composition and modal mineralogy may mask or oversimplify the details of granitoid petrogenesis. Finally, Neoproterozoic granitoid magmas in the JO provide no evidence of Neoproterozoic low $\delta^{18}O$ magmas as in Dabie–Sulu region.

Acknowledgments

This work was financially supported by the National Natural Science Foundation of China (Grant nos. 41072144 and 41222016), a 973 project of China (2012CB416701) and the US National Science Foundation (EAR-0319230, 0744079, 1053466) for SIMS time. Prof. J.W. Valley is greatly appreciated for thoughtful and helpful comments, discussions and corrections four times on earlier versions of the manuscript. We thank Q.L. Li and Y.R. Shi for ion microprobe U–Pb analyses at CAS-Beijing and CAGS-Beijing respectively, B. Wu for Laser U–Pb analyses at Nanjing University, J. Fournelle for CL and BSE images at UW-Madison, M. Spicuzza for laser fluorination oxygen isotope analyses at UW-Madison, T. Yang and A.J. Lin for Hf isotope analyses at Nanjing University. This manuscript benefited greatly from the thoughtful and constructive comments and suggestions from Prof. Calvin Miller and one anonymous reviewer.

Appendix A. Supporting information

Supplementary data associated with this article can be found in the online version at http://dx.doi.org/10.1016/j.epsl.2013.02.011.

References

Barth, A.P., Wooden, J.L., 2010. Coupled elemental and isotopic analyses of polygenetic zircons from granitic rocks by ion microprobe, with implications for melt evolution and the sources of granitic magmas. Chem. Geol. 277, 149–159.

Belousova, E.A., Griffin, W.L., O'Reilly, S.Y., Fisher, N.I., 2002. Igneous zircon: trace element composition as an indicator of source rock type. Contrib. Mineral. Petrol. 143, 602–622.

Bowman, J.R., Moser, D.E., Valley, J.W., Wooden, J.L., Kita, N.T., Mazdab, F.K., 2011. Zircon U–Pb isotope, $\delta^{18}O$ and trace element response to 80 m.y. of high temperature metamorphism in the lower crust: sluggish diffusion and new records of Archean craton formation. Am. J. Sci. 311, 719–772.

Chappell, B.W., White, A.J.R., 2001. Two contrasting granite types: 25 years later. Aust. J. Earth Sci. 48, 489–499.

Chen, R.X., Zheng, Y.F., Chen, R.X., Zhang, S.B., Li, Q.L., Dai, M.N., Chen, L., 2011. Metamorphic growth and recrystallization of zircons in extremely ^{18}O-depleted rocks during eclogite-facies metamorphism: evidence from U–Pb

ages, trace elements, and O–Hf isotopes. Geochim. Cosmochim. Acta 75, 4877–4898.
Chen, Z.H., Xing, G.F., Guo, K.Y., Dong, Y.G., Chen, R., Zeng, Y., Li, L.M., He, Z.Y., Zhao, L., 2009. Petrogenesis keratophyres in the Pingshui Group, Zhejiang: constraints from zircon U–Pb ages and Hf isotopes. Chin. Sci. Bull. 54, 1570–1578.
Claiborne, L.L., Miller, C.F., Wooden, J.L., 2010. Trace element composition of igneous zircon: a thermal and compositional record of the accumulation and evolution of a large silicic batholiths, Spirit Mountain, Nevada. Contrib. Mineral. Petrol. 160, 511–531.
Clemens, J.D., 2003. S-type granitic magmas-petrogenetic issues, models and evidence. Earth Sci. Rev. 61, 1–18.
Clemens, J.D., Stevens, G., 2012. What controls chemical variation in granitic magmas? Lithos 134–135, 317–329.
Collins, W.J., 1996. Lachlan Fold Belt granitoids: products of three-component mixing. Trans. R. Soc. Edinburgh, Earth Sci. 87, 171–181.
Ernst, W.G., Tsujimori, T., Zhang, R.Y., Liou, J.G., 2007. Permo-Triassic collision, subduction-zone metamorphism, and tectonic exhumation along the East Asian continental margin. Annu. Rev. Earth Planet. Sci. 35, 73–110.
Ferreira, V.P., Valley, J.W., Sial, A.N., Spicuzza, M.J., 2003. Oxygen isotope compositions and magmatic epidote from two contrasting metaluminous granitoids, NE Brazil. Contrib. Mineral. Petrol. 145, 205–216.
Fu, B., Kita, N.T., Wilde, S.A., Liu, X.C., Cliff, J., Greig, A., 2012. Origin of the Tongbai-Dabie-Sulu Neoproterozoic low-d18O igneous province, east-central China. Contrib. Mineral. Petrol., http://dx.doi.org/10.1007/s00410-012-0828-3, in press.
Goldstein, S.J., Jacobsen, S.B., 1988. Nd and Sr isotopic systematics of river water suspended material: implications for crustal evolution. Earth Planet. Sci. Lett. 87, 249–265.
Griffin, W.L., Belousova, E., Shee, S.R., Pearson, N.J., O'Reilly, S.Y., 2004. Archean crustal evolution in the northern Yilgarn Craton: U–Pb and Hf-isotope evidence from detrital zircons. Precambrian Res. 131, 231–282.
Hawkesworth, C.J., Kemp, A.I.S., 2006. Using hafnium and oxygen isotopes in zircons to unravel the record of crustal evolution. Chem. Geol. 206, 144–162.
Hoskin, P.W.O., Schaltegger, U., 2003. The composition of zircon and igneous and metamorphic petrogenesis. In: Hanchar, J.M., Hoskin, P.W.O. (Eds.), Zircon. Rev. Min. Geochem. 53, pp. 27–62.
Johannes, W., Holtz, F., 1996. Petrogenesis and Experimental Petrology of Granitic Rocks. Minerals and Rocks, vol. 20. Spring-Verlag, Berlin.
Kamei, A., 2002. Petrogenesis of Cretaceous Peraluminous granite suites with low initial Sr isotopic ratios, Kyushu Island, Southwest Japan Arc. Gondwana Res. 5, 813–822.
Kemp, A.I.S., Hawkesworth, C.J., Foster, G.L., Paterson, B.A., Woodhead, J.D., Hergt, J.M., Gray, C.M., Whitehouse, M.J., 2007. Magmatic and crustal differentiation history of granitic rocks from Hf–O isotopes in zircon. Science 315, 980–983.
Kemp, A.I.S., Hawkesworth, C.J., Collins, W.J., Gray, C.M., Blevin, P.L., EIMF, 2009. Isotopic evidence for rapid continental growth in an extensional accretionary orogen: the Tasmanides, eastern Australia. Earth Planet. Sci. Lett. 284, 455–466.
Lackey, J.S., Valley, J.W., Chen, J.H., Stockli, D.F., 2008. Dynamic magma systems, crustal recycling, and alteration in the Central Sierra Nevada Batholith: the oxygen isotope record. J. Petrol. 49, 1397–1426.
Li, S.G., Xiao, Y.L., Liu, D.L., Chen, Y.Z., Ge, N.J., Zhang, Z.Q., Sun, S.S., Cong, B.L., Zhang, R.Y., Hart, S.R., Wang, S.S., 1993. Collision of the North China and Yangtse Blocks and formation of coesite-bearing eclogites: timing and processes. Chem. Geol. 109, 89–111.
Li, X.H., 1999. U-Pb zircon ages of granites from the southern margin of the Yangtze margin: timing of Neoproterozoic Jinning Orogen in SE China and implication for Rodinia assembly. Precambrian Res. 97, 43–57.
Li, X.H., Li, Z.X., Ge, W.C., Zhou, H.W., Li, W.X., Liu, Y., Wingate, M.T.D., 2003. Neoproterozoic granitoids in South China: crustal melting above a mantle plume at *ca.* 825 Ma? Precambrian Res. 122, 45–83.
Li, X.H., Li, W.X., Li, Z.X., Lo, C.H., Wang, J., Ye, M.F., Yang, Y.H., 2009. Amalgamation between the Yangtze and Cathaysia Blocks in South China: constraints from SHRIMP U–Pb zircon ages, geochemistry and Nd–Hf isotopes of the Shuangxiwu volcanic rocks. Precambrian Res. 174, 117–128.
Li, Z.X., Li, X.H., Kinny, P.D., Wang, J., 1999. The breakup of Rodinia: did it start with a mantle plume beneath South China? Earth Planet. Sci. Lett. 173, 171–181.
Li, Z.X., Li, X.H., Kinny, P.D., Wang, J., Zhang, S., Zhou, H.W., 2003. Geochronology of Neoproterozoic syn-rift magmatism in the Yangtze Craton, South China and correlations with other continents: evidence for a mantle superplume that broke up Rodinia. Precambrian Res. 122, 85–109.
Miller, C.F., Watson, E.B., Harrison, T.M., 1988. Perspectives on the source, segregation, and transport of granitoid magmas. Trans. R. Soc. Edinburgh 79, 135–156.
Miller, C.F., McDowell, S.M., Mapes, R.W., 2003. Hot and cold granite? Implications of zircon saturation temperatures and preservation of inheritance. Geology 31, 529–532.
Page, F.Z., Ushikubo, T., Kita, N.T., Riciputi, L.R., Valley, J.W., 2007. High precision oxygen isotope analysis of picogram samples reveals 2-μm gradients and slow diffusion in zircon. Am. Mineral. 92, 1772–1775.
Qi, Q., Zhou, X.M., Wang, D.Z., 1986. The origin of the spilite-keratophyre series and the characteristic of the related mantle-derived granitic rocks in Xiqiu Zhejiang. Acta Petrol. Mineral. 5, 299–308. (in Chinese with English abstract).
Rudnick, R.L., Gao, S., 2003. Composition of the continental crust. In: Rudnick, R.L. (Ed.), The Crust, Treatise on Geochemistry, vol. 3. Elsevier, Amsterdam, pp. 1–64.
Solar, G.S., Pressley, R.A., Brown, M., Tucker, R.D., 1998. Granite ascent in contractional orogenic belts: testing a model. Geology 26, 711–714.
Spicuzza, M.J., Valley, J.W., McConnell, V.S., 1998. Oxygen isotope analysis of whole rock via laser fluorination: an air-lock approach. Geological Society of America, Abstracts with Programs 30, 80.
Valley, J.W., Kitchen, N., Kohn, M.J., Niendorf, C.R., Spicuzza, M.J., 1995. UWG-2, a garnet standard for oxygen isotope ratios: strategies for high precision and accuracy with laser heating. Geochim. Cosmochim. Acta 59, 5223–5231.
Valley, J.W., 2003. Oxygen isotopes in zircon. In: Hanchar, J.M., Hoskin, P.W.O. (Eds.), Zircon. Rev. Min. Geochem. 53, pp. 343–385.
Valley, J.W., Lackey, J.S., Cavosie, A.J., Clechenko, C.C., Spicuzza, M.J., Basei, M.A.S., Bindeman, I.N., Ferreira, V.P., Sial, A.N., King, E.M., Peck, W.H., Sinha, A.K., Wei, C.S., 2005. 4.4 billion years of crustal maturation: oxygen isotopes in magmatic zircon. Contrib. Mineral. Petrol. 150, 561–580.
Vavra, G., Schmid, R., Gebauer, D., 1999. Internal morphology, habit and U–Th–Pb microanalysis of amphibolite-to-granulite facies zircons: geochronology of the Ivrea Zone (Southern Alps). Contrib. Mineral. Petrol. 134, 380–404.
Vervoort, J.D., Blichert-Toft, J., 1999. Evolution of the depleted mantle: Hf isotope evidence from juvenile rocks through time. Geochim. Cosmochim. Acta 63, 533–556.
Wang, X.C., Li, Z.X., Li, X.H., Li, Q.L., Tang, G.Q., Zhang, Q.R., Liu, Y., 2011a. Nonglacial origin for low-δ^{18}O Neoproterozoic magmas in the South China Block: evidence from new *in-situ* oxygen isotope analyses using SIMS. Geology 39, 735–738.
Wang, X.C., Li, Z.X., Li, X.H., Li, Q.L., Zhang, Q.R., 2011b. Geochemical and Hf–Nd isotope data of Nanhua rift sedimentary and volcaniclastic rocks indicate a Neoproterozoic continental flood basalt provenance. Lithos 127, 427–440.
Wang, X.L., Zhou, J.C., Qiu, J.S., Zhang, W.L., Liu, X.M., Zhang, G.L., 2006. LA-ICP-MS U–Pb zircon geochronology of the Neoproterozoic igneous rocks from Northern Guangxi, South China: implications for petrogenesis and tectonic evolution. Precambrian Res. 145, 111–130.
Wang, X.L., Zhou, J.C., Griffin, W.L., Wang, R.C., Qiu, J.S., O'Reilly, S.Y., Xu, X.S., Liu, X.M., Zhang, G.L., 2007. Detrital zircon geochronology of Precambrian basement sequences in the Jiangnan orogen: dating the assembly of the Yangtze Cathaysia blocks. Precambrian Res. 159, 117–131.
Wang, X.L., Shu, L.S., Xing, G.F., Zhou, J.C., Tang, M., Shu, X., Qi, L., Hu, Y.H., 2012. Post-orogenic extension in the eastern part of the Jiangnan orogen: evidence from *ca.* 800–760 Ma volcanic rocks. Precambrian Res. 222–223, 404–423.
Wang, X.L., Griffin, W.L., Zhao, G., Zhou, J.C., Yu, J.H., Qiu, J.S., Zhang, Y.J., Xing, G.F. Understanding the contrasting geochemical features of crust in the Jiangnan orogen, submitted for publication.
White, A.J.R., Chappell, B.W., 1977. Ultrametamorphism and granitoid genesis. Tectonophysics 43, 7–22.
Wu, R.X., Zheng, Y.F., Wu, Y.B., Zhao, Z.F., Zhang, S.B., Liu, X.M., Wu, F.Y., 2006. Reworking of juvenile crust: element and isotope evidence from Neoproterozoic granodiorite in South China. Precambrian Res. 146, 179–212.
Xu, S.T., Okay, A.I., Ji, S.Y., Sengor, A.M.C., Su, W., Liu, Y.C., Jiang, L.L., 1992. Diamond from the Dabie Shan metamorphic rocks and its implication for tectonic setting. Science 256, 80–82.
Yang, J.H., Wu, F.Y., Chung, S.L., Wilde, S.A., Chu, M.F., 2004. Multiple sources for the origin of granites: geochemical and Nd/Sr isotopic evidence from the Gudaoling granite and its mafic enclaves, northeast China. Geochim. Cosmochim. Acta 68, 4469–4483.
Ye, M.F., 2006. SHRIMP U–Pb Zircon Geochronological, Geochemical and Nd–Hf–O Isotopic Evidences for Early Neoproterozoic Sibaoan Magmatic Arc Along the Southeastern Margin of Yangtze Block. Master's Degree Thesis. Graduate School of the Chinese Academy of Sciences. pp. 1–62 (in Chinese with English abstract).
Ye, M.F., Li, X.H., Li, W.X., Liu, Y., Li, Z.X., 2007. SHRIMP zircon U–Pb geochronological and whole-rock geochemical evidence for an early Neoproterozoic Sibaoan magmatic arc along the southeastern margin of the Yangtze Block. Gondwana Res. 12, 144–156.
Zheng, Y.F., Wu, Y.B., Chen, F.K., Gong, B., Li, L., Zhao, Z.F., 2004. Zircon U–Pb and oxygen isotope evidence for a large-scale ^{18}O depletion event in igneous rocks during the Neoproterozoic. Geochim. Cosmochim. Acta 68, 4145–4165.
Zheng, Y.F., Wu, Y.B., Zhao, Z.F., Zhang, S.B., Xu, P., Wu, F.Y., 2005. Metamorphic effect on zircon Lu–Hf and U–Pb isotope systems in ultrahigh-pressure eclogite-facies metagranite and metabasite. Earth Planet. Sci. Lett. 240, 378–400.
Zheng, Y.F., Wu, R.X., Wu, Y.B., Zhang, S.B., Yuan, H.L., Wu, F.Y., 2008. Rift melting of juvenile arc-derived crust: geochemical evidence from Neoproterozoic volcanic and granitic rocks in the Jiangnan orogen, South China. Precambrian Res. 163, 351–383.
Zhou, X.M., Wang, D.Z., 1988. The peraluminous granodiorites with low initial ^{87}Sr/^{86}Sr ratio and their genesis in southern Anhui Province, eastern China. Acta Petrol. Sin. 4, 37–45. (in Chinese with English abstract).
Zhu, D.C., Mo, X.X., Niu, Y.L., Zhao, Z.D., Yang, Y.H., Wang, L.Q., 2009. Zircon U–Pb dating and *in-situ* Hf isotopic analysis of Permian peraluminous granite in the Lhasa terrane, southern Tibet: implications for Permian collisional orogeny and paleogeography. Tectonophysics 469, 48–60.
Zhu, D.C., Zhao, Z.D., Niu, Y.L., Mo, X.X., Chung, S.L., Hou, Z.Q., Wang, L.Q., Wu, F.Y., 2011. The Lhasa Terrane: record of a microcontinent and its histories of drift and growth. Earth Planet. Sci. Lett. 301, 241–255.